

Regiospecific Analysis of Diricinoleoylglycerols in Castor (*Ricinus communis L.*) Oil by Electrospray Ionization–Mass Spectrometry

JIANN-TSYH LIN* AND ARTHUR ARCIÑAS

Western Regional Research Center, Agricultural Research Service, U.S. Department of Agriculture,
800 Buchanan Street, Albany, California 94710

HPLC fractions of diricinoleoylglycerols containing one non-ricinoleoyl chain from castor oil were used to identify the regiospecific location of this non-ricinoleoyl chain on the glycerol backbone using electrospray ionization–MS³ of lithium adducts. The regiospecific ions used were from the loss of α,β -unsaturated fatty acid specific at the *sn*-2 position. The content of 1,3-diricinoleoyl-2-oleoyl-*sn*-glycerols (ROR) among the three stereospecific isomers, RRO, ROR and ORR, was about 91%. The contents of other 1,3-diricinoleoyl-2-acyl-glycerols among the three stereospecific isomers were as follows: 1,3-diricinoleoyl-2-linoleoyl-*sn*-glycerol, 95%; 1,3-diricinoleoyl-2-linolenoyl-*sn*-glycerol, 96%; 1,3-diricinoleoyl-2-stearoyl-*sn*-glycerol, 96%; 1,3-diricinoleoyl-2-palmitoyl-*sn*-glycerol, 78%; and 1,3-diricinoleoyl-2-lesqueroloyl-*sn*-glycerol, 31%. These non-hydroxyl fatty acids were mostly at the *sn*-2 position of triacylglycerols in castor oil. These results suggest that phospholipase A₂ hydrolysis of phosphatidylcholine (PC) containing non-hydroxyl fatty acid at the *sn*-2 position is either blocked or partially blocked in vivo. Phospholipase A₂ hydrolysis of 2-lesqueroloyl-PC is not blocked and is similar to that of 2-ricinoleoyl-PC. Transgenic inhibition of phospholipase C hydrolysis of PC might be used to block the incorporation of non-hydroxyl fatty acids into triacylglycerols, thus increasing the content of ricinoleate in seed oil.

KEYWORDS: Castor oil; ricinoleate; triacylglycerols; diricinoleoyl-*sn*-glycerol; diricinoleoylglycerols; regiospecific analysis; LC-MS; phospholipase A₂; phospholipase C; *Ricinus communis L.*

INTRODUCTION

Ricinoleate (R), a hydroxy fatty acid (FA), has many industrial uses including the manufacture of aviation lubricant, plastics, paints, and cosmetics. Ricinoleate occurs as acylglycerols (AG) and constitutes about 90% of the fatty acids in castor oil (1). Castor oil is the only commercial source of ricinoleate. However, castor bean contains the toxin, ricin, and potent allergens, which make it hazardous to grow, harvest, and process. It would be desirable to produce ricinoleate from a transgenic oilseed lacking these toxic components. The biosynthetic pathway of triricinolein (RRR) and (12-ricinoleoylricinoleoyl)diricinoleoylglycerol (RRRR) in castor bean has been established, and the key enzymatic steps driving ricinoleate into RRR and RRRR have been identified (2–5) (Figure 1). This information can be used to develop transgenic plants that produce seed oil containing RRR and RRRR without the aforementioned toxic substances. With the identification of RRRR in castor oil (5), it is desirable to overproduce RRRR in transgenic seed because of its higher ricinoleate content compared to that of RRR. The key enzymatic steps identified were lysophosphatidylcholine acyltransferase (incorporates ole-

ate) (4), oleoyl-12-hydroxylase, phospholipase A₂, and diacylglycerol acyltransferase (2). 2-Oleoylphosphatidylcholine (PC) is the direct precursor of 2-ricinoleoyl-PC, the substrate for oleoyl-12-hydroxylase (2). The cDNA for oleoyl-12-hydroxylase, the enzyme catalyzing the hydroxylation of oleate to ricinoleate, has been cloned from castor and expressed in tobacco, resulting in accumulation of low levels of ricinoleate in seed oil (6). Expression of this enzyme in transgenic *Arabidopsis thaliana* resulted in improved but still low amounts of hydroxy FA (7) compared to castor oil (20% vs 90% ricinoleate in castor oil).

We have identified and quantified 16 molecular species of AG in castor oil by C₁₈ HPLC and evaporative light scattering detector (ELSD) (1). The content of RRR in castor oil was 71%. The contents of diricinoleoylglycerols (RRAc) containing non-ricinoleoyl chains are as follows: diricinoleoyl-*sn*-glycerol (RRO, 7.2%), diricinoleoyl-linoleoylglycerol (RRL, 6.6%), diricinoleoyl-linolenoylglycerol (RRLn, 0.15%), diricinoleoyl-stearoylglycerol (RRS, 1.1%), diricinoleoylpalmitoylglycerol (RRP, 1.6%), and diricinoleoyl-lesqueroloylglycerol (RRLs, 0.7%). The identity of these molecular species of AG in castor oil has been confirmed recently by LC-ESI-MS (5). We are interested in knowing the stereospecific locations of the non-ricinoleoyl chains in these RRAs, because this will help to

* Author to whom correspondence should be addressed [telephone (510) 559-5764; fax (510) 559-5768; e-mail jlin@pw.usda.gov].

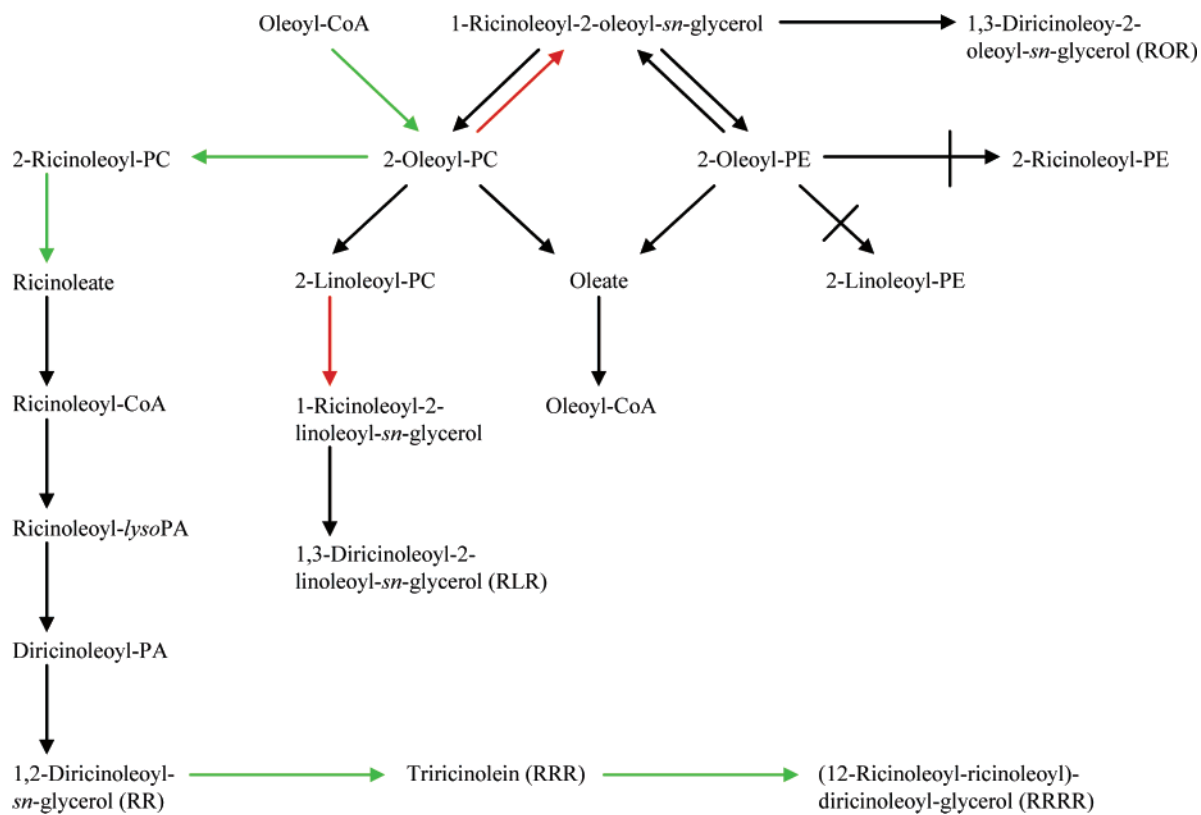


Figure 1. Proposed biosynthetic pathway of castor oil. Green arrows show the key enzyme steps driving ricinoleate into acylglycerols. Two arrows with solid bars show a complete block. Red arrows show the phospholipase C hydrolysis, which can be targeted to block the incorporation of non-hydroxyl fatty acids into triacylglycerols to increase presumably the content of ricinoleate in transgenic seed oils.

interpret the biosynthetic pathway and predict the physical properties of castor oil relevant to industrial uses. The regiospecific characterization of triacylglycerols (TAG) as lithiated adducts by collisionally activated dissociation tandem mass spectrometry (CAD-MS²) has been reported (8). We used a similar technique, MS³, to determine the regiospecific location of non-ricinoleoyl acyl groups (Ac) in RRAc.

EXPERIMENTAL PROCEDURES

Materials. Castor oil and lithium acetate were obtained from Sigma. Fisher brand HPLC grade solvents for chromatographic separation and Burdick & Jackson GC-MS grade methanol and isopropanol for LC-MS were purchased from Fisher Scientific. High-purity nitrogen and helium gas for LC-MS were acquired from Praxair (Oakland, CA).

HPLC Fractionation of the Molecular Species of TAGs in Castor Oil. The fractionation of the molecular species of TAGs in castor oil was the same as previously reported for the fractionation and collection of RRR and RRRR (5). The chromatograms showing the fractionation of RRLs, RRLn, RRL, RRP, RRO, and RRS in castor oil have been published (1, 5). Chromatographic fractionation was performed using a Waters HPLC (Waters Associates, Milford, MA) and a C₁₈ column (Gemini, 250 × 4.6 mm, 5 μm, C18, Phenomenex, Torrance, CA). One milligram of castor oil was chromatographed at 22 °C with a linear gradient from 100% methanol to 100% 2-propanol in 40 min, at a 1 mL/min flow rate, and detected at 205 nm (9, 10). Half-minute fractions were collected, and analogous fractions were pooled from six runs. The six RRAc and their fractions collected for MS analysis were as follows: RRLs (fraction 21), RRLn (fractions 26 and 27), RRL (fractions 29 and 30), RRP (fraction 32), RRO (fractions 32 and 33), and RRS (fractions 36 and 37). Fractions were evaporated to dryness with nitrogen gas at 22 °C using a Pierce Reacti-Vap (Rockford, IL) evaporation unit. The residues were redissolved in 1.5 mL of methanol containing 20 mM lithium acetate. TAG concentrations were calculated using previous ELSD data obtained from HPLC separations (5).

ESI-MS³ of the Fraction Collected Diricinoleylacylglycerols (RRAc). An LCQ Advantage ion-trap mass spectrometer with Xcalibur 1.3 software (ThermoFinnigan, San Jose, CA) was utilized for MS³ analysis of the various RRAc fractions collected from castor oil (5). Direct infusion of 200 μL samples into MS at a 2.5 μL/min flow rate from a syringe pump produced stable singly charged parent ions, which were subsequently fragmented for MS² and MS³ analysis. ESI source conditions were as follows: 50 arbitrary units (au) of nitrogen (Praxair) sheath gas flow rate, 4.5 kV spray voltage, 250 °C capillary temperature, isolation width of *m/z* 1.0 or 1.5, mass range of *m/z* 300–2000, acquisition time of 3 min, capillary voltage of 38 V, and normalized collision energy ranging from 36 to 41% for both MS² and MS³ fragmentations, varying between TAG samples. Research grade (99.999%) helium was used as collision gas.

RESULTS AND DISCUSSION

HPLC fractionation of TAG in castor oil was the same as we reported recently (5). The fractions collected, RRLs, RRLn, RRL, RRP, RRO, and RRS, in elution order, were analyzed by ESI-MS³ as lithium adducts. RRP eluted slightly earlier than RRO, which is the reverse order from earlier reports (9, 10) that “P” species of TAG elutes slightly later than the “O” species of the TAG, with all else equal. The TAG of earlier reports did not contain ricinoleate. The relative retention times of TAG-containing ricinoleate have been reported (11).

The MS² spectrum of [RRO + Li]⁺ at *m/z* 923.7 (Figure 2) shows the precursor ion and the fragment ions of [RRO + Li - RCOOH]⁺ at *m/z* 625.5 and [RRO + Li - OCOOH]⁺ at *m/z* 641.5, reflecting the neutral losses of ricinoleic acid (RCOOH) and oleic acid (OCOOH), respectively. The structures of these fragment ions have been proposed to contain a 1,3-dioxolane ring (five-membered ring) with the two carbon atoms on the ring from the glycerol backbone (8). Unlike the previous

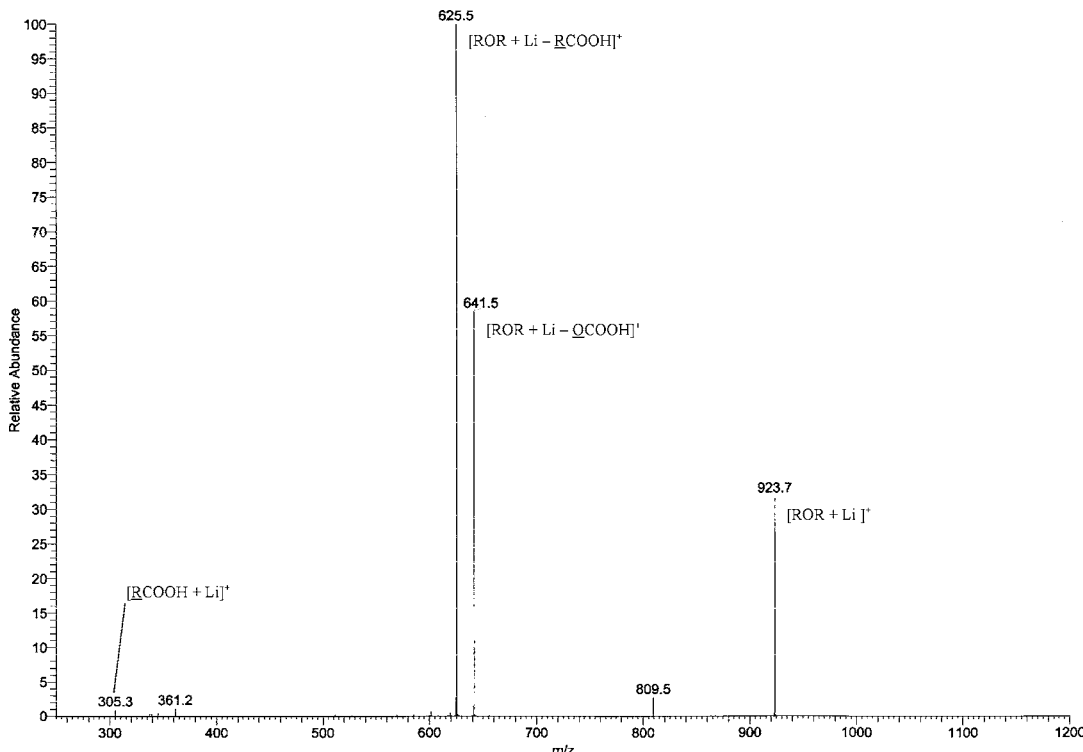


Figure 2. Ion trap mass spectrum of ESI-MS² of $[ROR + Li]^{+}$ ion at m/z 923.7. Both R and \underline{RCOOH} are ricinoleic acid. Both O and \underline{OCOOH} are oleic acid. ROR is diricinoleoyl-oleoyl-glycerol (non-stereospecific) from castor oil including RRO and ORR if any.

paper (8), the neutral loss of the lithium salts of these fatty acids from $[RRO + Li]^{+}$ was not observed as $[RRO + Li - (RCOOLi)]^{+}$ and $[RRO + Li - (OOLi)]^{+}$. The other non-lithiated adducts, for example, \underline{RCO}^{+} , $\underline{RCO}^{+} - 18$, \underline{OCO}^{+} , $\underline{OCO}^{+} - 18$, shown earlier (8) were also not observed here, yielding a much simpler spectrum (Figure 2). The difference appearing in the spectra might be due to the different methods used. The earlier report (8) used a tandem sector quadrupole instrument with “in-source” CAD, whereas we used an ion-trap instrument.

Ricinoleate, $[\underline{RCOOH} + Li]^{+}$ at m/z 305.2, was detected slightly (Figure 2). Oleate, $[\underline{OCOOH} + Li]^{+}$ at m/z 289.3, was not detected. In a recent report of MS² spectra of sodium adducts of $[RRRR + Na]^{+}$ at m/z 1236.0 from (12-ricinoleoylricinoleoyl)diricinoleoylglycerol (RRRR) and $[RRR + Na]^{+}$ at m/z 955.7 from triricinolein (RRR) (5), we detected the free fatty acid, $[\underline{RCOOH} + Na]^{+}$ at m/z 321.2 and $[\underline{RCOOR} \underline{COOH} + Na]^{+}$ at m/z 601.5 from RRRR. For the purpose of detecting free fatty acids in MS² spectra of acylglycerols, sodium adducts yielded improved fragmentation in comparison to lithium and ammonium adducts.

Figure 3 shows the MS³ spectrum of $[ROR + Li - \underline{RCOOH}]^{+}$ at m/z 625.5. Regiospecific ions were derived from the loss of α,β -unsaturated fatty acids specific at the *sn*-2 position (8) and were the two ions of $[ROR + Li - \underline{RCOOH} - \underline{O'CH=CHCOOH}]^{+}$ at m/z 345.2 and $[RRO \text{ and/or } ORR + Li - \underline{RCOOH} - \underline{R'CH=CHCOOH}]^{+}$ at m/z 329.3. The abundance of the latter ion was very low (Figure 3). It seems that the oleoyl moiety of ROR (non-stereospecific) in castor oil was mostly at the *sn*-2 position according to the relative abundances of m/z 345.2 and 329.3. However, most of the ion at m/z 345.2 was from $[ROR + Li - \underline{RCOOH} - \underline{R'CH=CHCOOH}]^{+}$, not $[ROR + Li - \underline{RCOOH} - \underline{O'CH=CHCOOH}]^{+}$. The ratio of these two ions and identification of the ion resulting from the loss of ketene will be given in a later

section. The fragmentation pathway of the loss of α,β -unsaturated fatty acids specific at the *sn*-2 position has been proposed previously by Hsu and Turk as shown in Figure 4A (8).

Figure 3 also shows ricinoleate, $[\underline{RCOOH} + Li]^{+}$ at m/z 305.3, and oleate, $[\underline{OCOOH} + Li]^{+}$ at m/z 289.2, to a lesser extent. A major ion $[ROR + Li - \underline{RCOOH} - C_7H_{14}O]^{+}$ at m/z 511.4 was formed from the cleavage between C-11 and C-12 of the ricinoleoyl chain next to the hydroxyl group. The hydrogen atom of the hydroxyl group migrated to this lithium adduct during fragmentation. A major ion at m/z 569.3 (Figure 3) may be the acid anhydride of ricinoleate and oleate, $[\underline{RCOOCOO} + Li]^{+}$, and is the same as $[ROR + Li - \underline{RCOOH} - C_3H_4O]^{+}$. The proposed fragmentation pathway for $[ROR + Li - \underline{RCOOH} - C_3H_4O]^{+}$ is shown in Figure 4B, with the intermediate containing a 1,3-dioxolane five-membered ring with the two carbon atoms of the ring originating from the glycerol backbone. C_3H_4O is the same as $CH_2=CHCHO$ from the glycerol backbone of the TAG. The ion from the loss of glycerol and formation of acid anhydride from the two fatty acids has not been reported previously. In addition to the acid anhydride, it is also possible that the structure of m/z 569.3 was similar to that of acid anhydride shown in Figure 4B except the location of the double bond. Instead of the double bond at the keto group, the double bond was at the C-1 position (carbon–carbon double bond) of the same acyl chain and the keto group became a hydroxyl group. The double bond at C-2 as α,β -unsaturated fatty acids was also possible for the ion at m/z 569.3.

Figure 5 shows the MS³ spectrum of $[ROR + Li - \underline{OCOOH}]^{+}$ at m/z 641.5. The relative abundance of the ion at m/z 345.2, $[RRO \text{ and/or } ORR + Li - \underline{OCOOH} - \underline{R'CH=CHCOOH}]^{+}$, resulting from the loss of α,β -unsaturated ricinoleic acid specific at the *sn*-2 position, was low compared to those of the five major ions. However, this ion was still

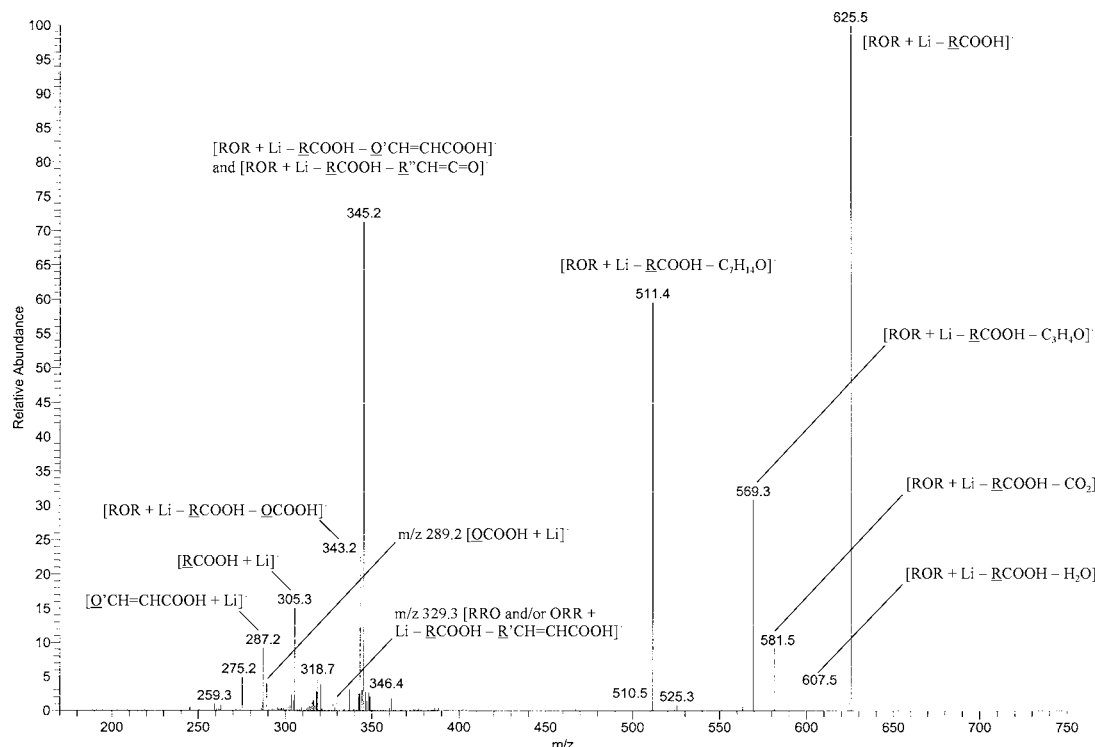


Figure 3. Ion trap mass spectrum of ESI-MS³ of $[ROR + Li - ROOH]^+$ at m/z 625.5. For abbreviations, see **Figure 2**. $O'CH=CHCOOH$ is α,β -unsaturated oleic acid from the *sn*-2 position. $R'CH=CHCOOH$ is α,β -unsaturated ricinoleic acid from the *sn*-2 position. $C_7H_{14}O$ is the loss from the cleavage between C-11 and C-12 of ricinoleate chain. C_3H_4O is the loss of glycerol backbone to form acid anhydride of two fatty acids. $R''CH=C=O$ is a ketene from ricinoleate at the *sn*-1,3 position.

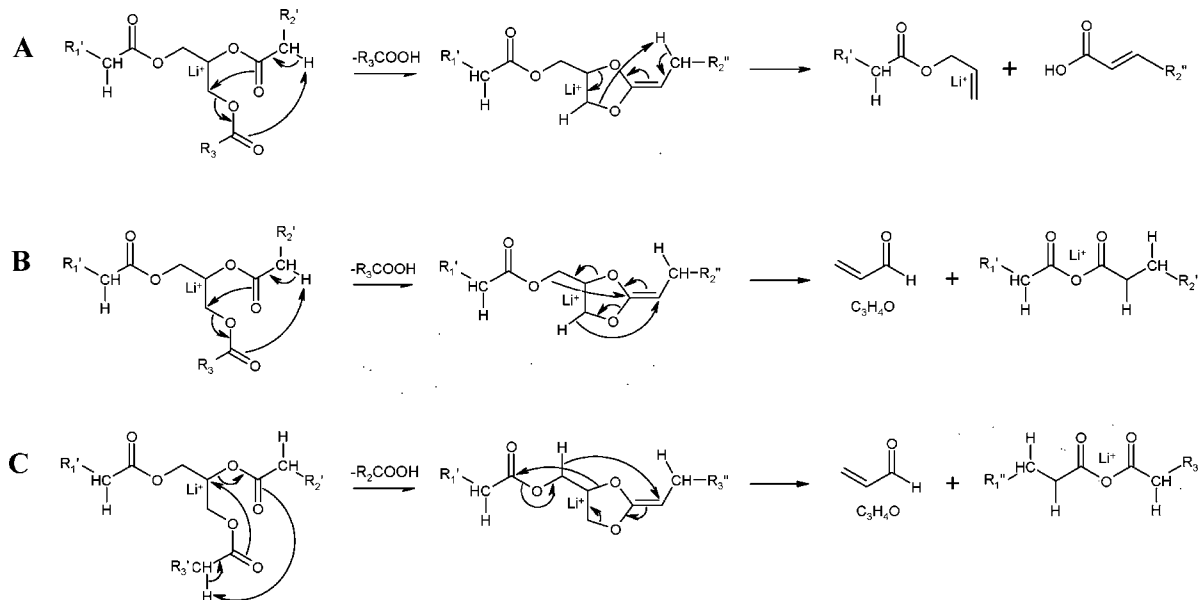


Figure 4. Proposed fragmentation pathways of triacylglycerol lithium adducts by ESI-MS³: (A) loss of fatty acid at *sn*-3, then the loss of α,β -unsaturated fatty acid at *sn*-2 [proposed by Hsu and Turk (8)]; (B) loss of fatty acid at *sn*-3, then the loss of C_3H_4O from glycerol backbone to form acid anhydride; (C) loss of fatty acid at *sn*-2, then the loss of C_3H_4O from glycerol backbone to form acid anhydride. R = fatty acid. Subscripts after R represent the stereospecific locations.

significant; thus, RRO and ORR are present in castor oil. Ricinoleate, $[RCOOH + Li]^+$ at m/z 305.3, was one of the major ions. As expected, oleate, $[OCOOH + Li]^+$ at m/z 289.3, was not present.

$[ROR + Li - OCOOH - R''CH=C=O]^+$ at m/z 361.2 occurred as a major ion (**Figure 5**), whereas $[RRO \text{ and/or } ORR + Li - RCOOH - O''CH=C=O]^+$ at m/z 361.2 was a minor ion (**Figure 3**). These results indicate that loss of $R''CH=C=O$

$=O$ and $OOCCH=C=O$ were regiospecific and bound to the *sn*-1 and/or *sn*-3 positions (8) and that the contents of RRO and ORR were very low.

The ion at m/z 527.3 (**Figure 5**), $[ROR + Li - OCOOH - C_7H_{14}O]^+$, was from the cleavage between C-11 and C-12 adjacent to the hydroxyl group of the ricinoleyl chain. The major ion at m/z 585.4 might be the acid anhydride of ricinoleic acid, $[RCOOCOR + Li]^+$, and was the same as $[ROR + Li -$

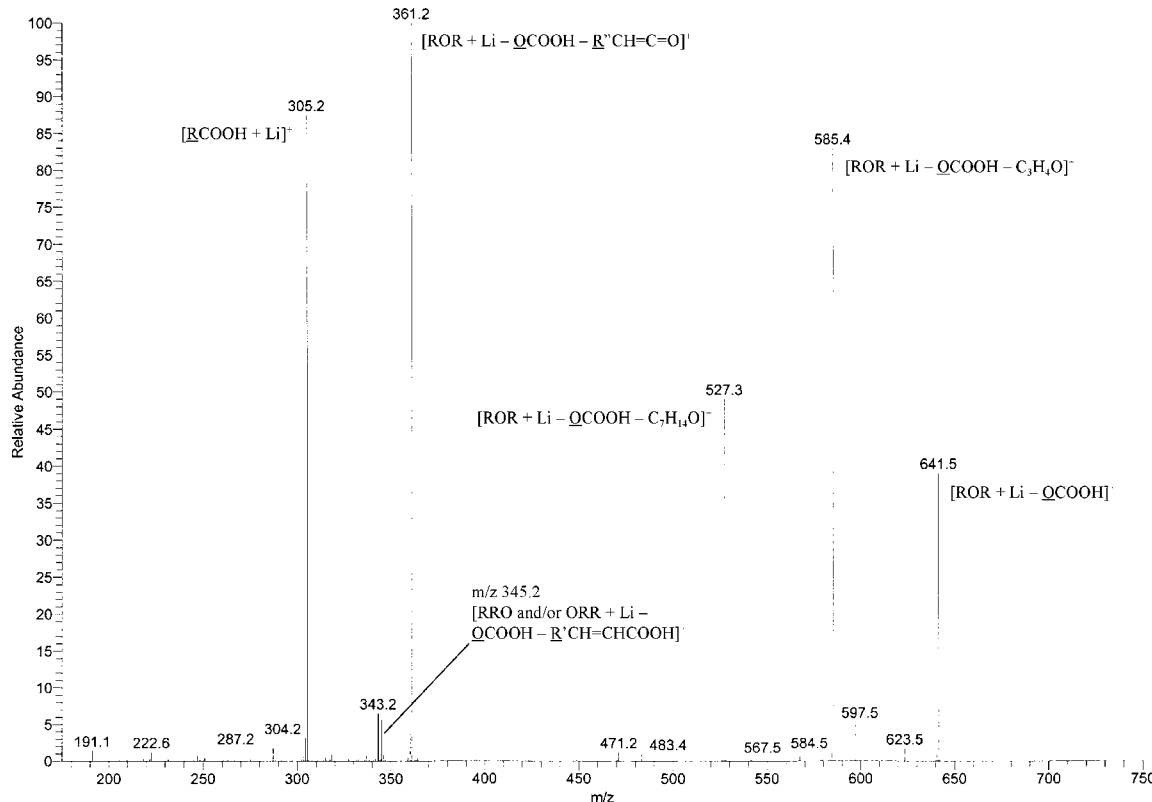


Figure 5. Ion trap mass spectrum of ESI-MS³ of $[ROR + Li - \underline{OCOOH}]^+$ at m/z 641.5. For abbreviations, see Figures 2 and 3.

$\underline{OCOOH} - C_3H_4O]^+$. The loss of C_3H_4O , m/z 56, is also shown in Figure 3 at m/z 569.4. The proposed fragmentation pathway for $[ROR + Li - \underline{OCOOH} - C_3H_4O]^+$ is shown as Figure 4C.

Figure 6 shows the MS³ spectrum of $[RLR + Li - \underline{RCOOH}]^+$ at m/z 623.5. Figure 7 shows the MS³ spectrum of $[RLnR + Li - \underline{RCOOH}]^+$ at m/z 621.5. The fragmentation pattern shown in these two MS³ spectra is similar to that given in Figure 3. Figure 7 shows the three different ions, $[RLnR + Li - \underline{RCOOH} - R''CH=C=O]^+$ at m/z 341.2, $[RLnR + Li - \underline{RCOOH} - \underline{LnCOOH}]^+$ at m/z 343.2, and $[RLnR + Li - \underline{RCOOH} - \underline{Ln'}CH=CHCOOH]^+$ at m/z 345.3, and these three m/z values are different. Figure 6 shows both of the ions $[RLR + Li - \underline{RCOOH} - R''CH=C=O]^+$ and $[RLR + Li - \underline{RCOOH} - \underline{LCOOH}]^+$ at m/z 343.2. These two ions are not isotopic with the ion used for the regiospecific identification, $[RLR + Li - \underline{RCOOH} - \underline{L'}CH=CHCOOH]^+$ at m/z 345.3.

In Figure 3, most of the ion at m/z 345.2 was from $[ROR + Li - \underline{RCOOH} - R''CH=C=O]^+$, not $[ROR + Li - \underline{RCOOH} - \underline{O''CH=CHCOOH}]^+$ because Figure 7 showed that the abundance of $[RLnR + Li - \underline{RCOOH} - R''CH=C=O]^+$ was almost 4 times of that of $[RLnR + Li - \underline{RCOOH} - \underline{Ln'}CH=CHCOOH]^+$. Hsu and Turk (8) did not mention the loss of the ketene from lithiated TAGs and mentioned only the loss of the α,β -unsaturated fatty acids. However, in this paper the losses of ricinoleate ketene at *sn*-1,3 positions were major ions. All of the major ions from the loss of ketene in Figures 3 and 5–7 were from the loss of ricinoleate ketene. The hydroxyl group on ricinoleate and the methods used made the difference. This is the first report of the MS of lithiated TAG containing ricinoleate. Neutral loss of ketene at the *sn*-3 position was proposed by Cheng et al. as $[RCO + 74]^+$ (12) on the CAD spectra of ESI-produced $[M + NH_4]^+$.

The MS³ spectra of $[RSR + Li - \underline{RCOOH}]^+$ at m/z 627.5, $[RPR + Li - \underline{RCOOH}]^+$ at m/z 599.5, and $[RLsR + Li - \underline{RCOOH}]^+$

$\underline{RCOOH}]^+$ at m/z 669.5 were also obtained. These spectra were similar to those shown in Figures 3, 6, and 7. The ions due to the loss of α,β -unsaturated fatty acids specific at the *sn*-2 position, $[RSR + Li - \underline{RCOOH} - S'CH=CHCOOH]^+$ at m/z 345.3, $[RPR + Li - \underline{RCOOH} - P'CH=CHCOOH]^+$ at m/z 345.3, and $[RLsR + Li - \underline{RCOOH} - Ls'CH=CHCOOH]^+$ at m/z 345.3, were different from the ions of $[RSR + Li - \underline{RCOOH} - R''CH=C=O]^+$ at m/z 347.3, $[RPR + Li - \underline{RCOOH} - R''CH=C=O]^+$ at m/z 319.2, and $[RLsR + Li - \underline{RCOOH} - R''CH=C=O]^+$ at m/z 389.3. Therefore, the relative abundance of the ions resulting from the loss of the α,β -unsaturated fatty acids specific at the *sn*-2 position can be estimated directly.

The contents of RAcR among RRAc, RAcR, and AcRR combined were estimated by the comparison of relative abundances of the two ions $[RAcR + Li - \underline{RCOOH} - Ac'CH=CHCOOH]^+$ and $[RRAc + Li - \underline{RCOOH} - R'CH=CHCOOH]^+$ as shown in Figures 3, 6, and 7. Among the 12 ions used from the six RRAc in castor oil, only the ion $[ROR + Li - \underline{RCOOH} - \underline{O'CH=CHCOOH}]^+$ at m/z 345.2 in Figure 3 was mixed with the ion from the loss of ketene, $[ROR + Li - \underline{RCOOH} - R'CH=C=O]^+$ at m/z 345.2. The relative abundance of $[ROR + Li - \underline{RCOOH} - \underline{O'CH=CHCOOH}]^+$ was estimated from the ratios of the three ions $[RLnR + Li - \underline{RCOOH} - R''CH=C=O]^+$ at m/z 341.2, $[RLnR + Li - \underline{RCOOH} - \underline{LnCOOH}]^+$ at m/z 343.2, and $[RLnR + Li - \underline{RCOOH} - \underline{Ln'}CH=CHCOOH]^+$ at m/z 345.3 in Figure 7. The relative abundance of $[ROR + Li - \underline{RCOOH} - \underline{O'CH=CHCOOH}]^+$ was then compared with that of $[ROR + Li - \underline{RCOOH} - R''CH=C=O]^+$ at m/z 325.3 to get the content of ROR. When the ratio of the abundances of $[RLnR + Li - \underline{RCOOH} - \underline{LnCOOH}]^+$ at m/z 343.2 and $[RLnR + Li - \underline{RCOOH} - \underline{Ln'}CH=CHCOOH]^+$ at m/z 345.2 in Figure 7 was used, the content of ROR among the three isomers (ROR, RRO, and ORR) combined was 88%. When the ratio of the abun-

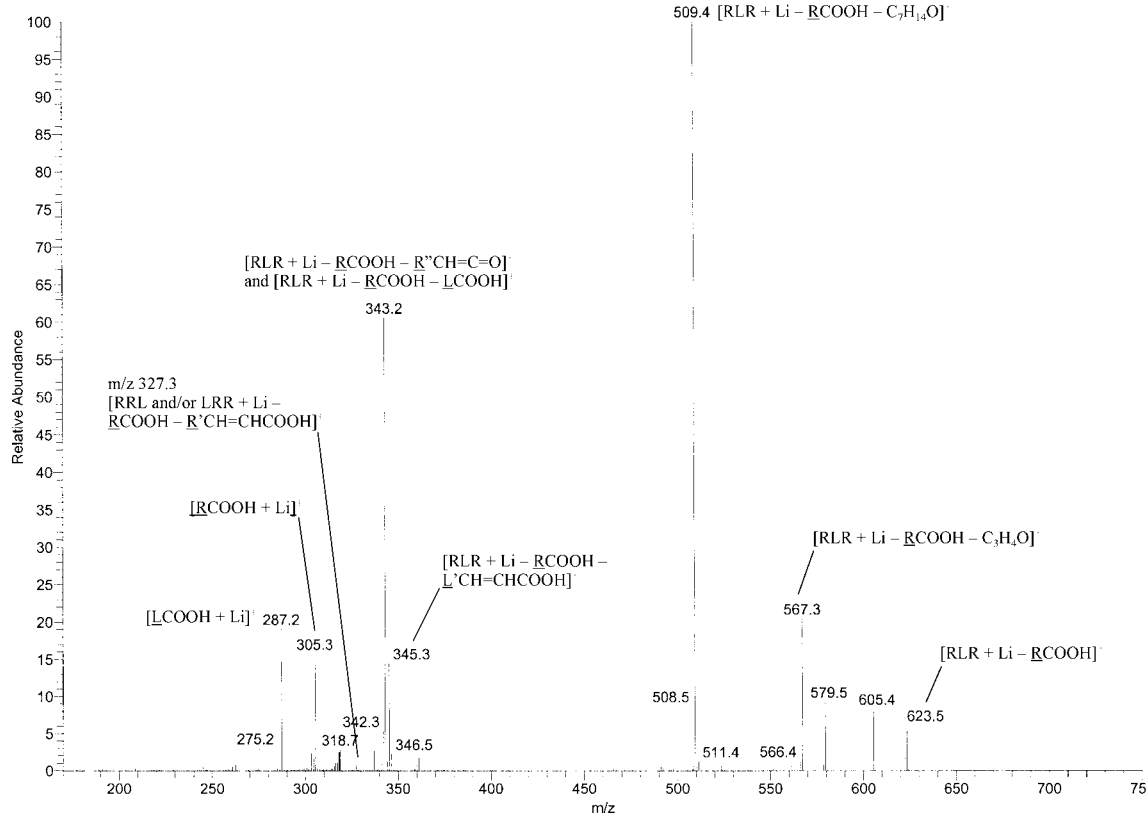


Figure 6. Ion trap mass spectrum of ESI-MS³ of $[RLR + Li - RCOOH]^+$ at m/z 623.5. For abbreviations, see **Figures 2** and **3**. $\underline{L}'CH=CHCOOH$ is α,β -unsaturated linoleic acid from the *sn*-2 position. Both L and $\underline{L}'COOH$ are linoleic acid. RLR here is diricinoleoyl-linoleoyl-glycerol (non-stereospecific) from castor oil including RRL and LRR if any.

dances of $[RLnR + Li - RCOOH - R''CH=C=O]^+$ at m/z 341.2 and $[RLnR + Li - \underline{R}'COOH - \underline{L}'CH=CHCOOH]^+$ at m/z 345.3 in **Figure 7** was used, the content of ROR among the three isomers (ROR, RRO, and ORR) combined was 91%. We prefer to use the latter, because it avoided the use of the third ion for calculation.

From the relative abundances of the two ions derived from the loss of α,β -unsaturated fatty acids specific at the *sn*-2 position for each of the other RRAc in castor oil, we estimated the content of the 1,3-diricinoleoyl-2-acyl-*sn*-glycerol species among the three isomers as follows: RLR, 95%; RLnR, 96%; RSR, 96%; RPR, 78%; and RLsR, 31%. These values fall consistently within $\pm 3\%$ in repeated experiments. Both MS³ and CAD-MS² were used to measure the content of each 1,3-diricinoleoyl-2-acyl-*sn*-glycerol among the three possible stereoisomers with equivalent results (data not shown).

Regioisomers in vegetable oils (13) and in animal fats (14) have been identified by atmospheric pressure chemical ionization-mass spectrometry (APCI-MS) based on the premise that the loss of the acyl group from the *sn*-1 or *sn*-3 position is energetically favored over the loss from the *sn*-2 position. The ratios of the regiospecific isomers can be determined from a linear calibration curve of the ratio of $[LL]^+$ and $[LO]^+$ derived from various concentrations of regiospecific LOL and LLO standards by APCI-MS (15, 16). We cannot use this method to determine the ratios of regioisomers of diricinoleoylacylglycerols because of a lack of the regiospecific standards. In addition, the very minor regioisomers cannot be positively identified by this method, because both LOL and LLO produce both $[LL]^+$ and $[LO]^+$. ESI-MS³ of lithium adducts detects ions from the loss of α,β -unsaturated fatty acid specific at the *sn*-2 position, so the very minor regioisomers can be identified, such as $[RRO + Li - RCOOH - R'CH=CHCOOH]^+$ at m/z 329.3 (Figure 3), $[RRO$ and/or $ORR + Li - OCOOH - R'CH=CHCOOH]^+$ at m/z 345.2 (Figure 5), $[RRL$ and/or $LRR + Li - RCOOH - R'CH=CHCOOH]^+$ at m/z 327.3 (Figure 6), and $[RRLn$ and/or $LnRR + Li - RCOOH - R'CH=CHCOOH]^+$ at m/z 325.3 (Figure 7). We assume a linear relationship of the ion response and the amount of isomer as reported earlier (15).

The ratio $[RR]^+/[OR]^+$ from ROR (about 91% regiospecifically pure) shown in **Figure 2** was 58%. This did not agree with the previous report (8) that the ratio of $[AA]^+/[AB]^+$ from ABA obtained from the regiospecific SOS and POP standards was about 1:3 (or 33%). The disagreement might be because ROR contained hydroxy fatty acids and the ratio of $[AA]^+/[AB]^+$ from ROR using the current method resulted in different ratios. The ratio of $[RR]^+/[LR]^+$ from RLR (about 95% regiospecifically pure) was 50%, and the ratio of $[RR]^+/[LnR]^+$ from RLnR (about 96% regiospecifically pure) was 52%. These two ratios were similar to those from ROR.

Oleate of oleoyl-CoA is incorporated into 2-oleoylphosphatidylcholine (2-oleoyl-PC) by lysophosphatidylcholine-acyltransferase and then hydroxylated to 2-ricinoleoyl-PC by 12-oleoylhydroxylase in castor microsomes (Figure 1) (2, 5). 2-Oleoyl-PC is also desaturated to 2-linoleoyl-PC and then to 2-linolenoyl-PC (2). Various fatty acids can be incorporated at different rates into PC by lysophosphatidylcholine-acyltransferase (4). These 2-non-ricinoleoyl-PC are converted to 1,3-diricinoleoyl-2-nonricinoleoyl-*sn*-glycerol (RAcR) through reactions catalyzed by phospholipase C and then diacylglycerol acyltransferase (DGAT). Among these RAcR, only ROR and RLR, the most abundant RAcR in castor oil, are shown in **Figure 1**. PC can be hydrolyzed by phospholipase A₂ to release

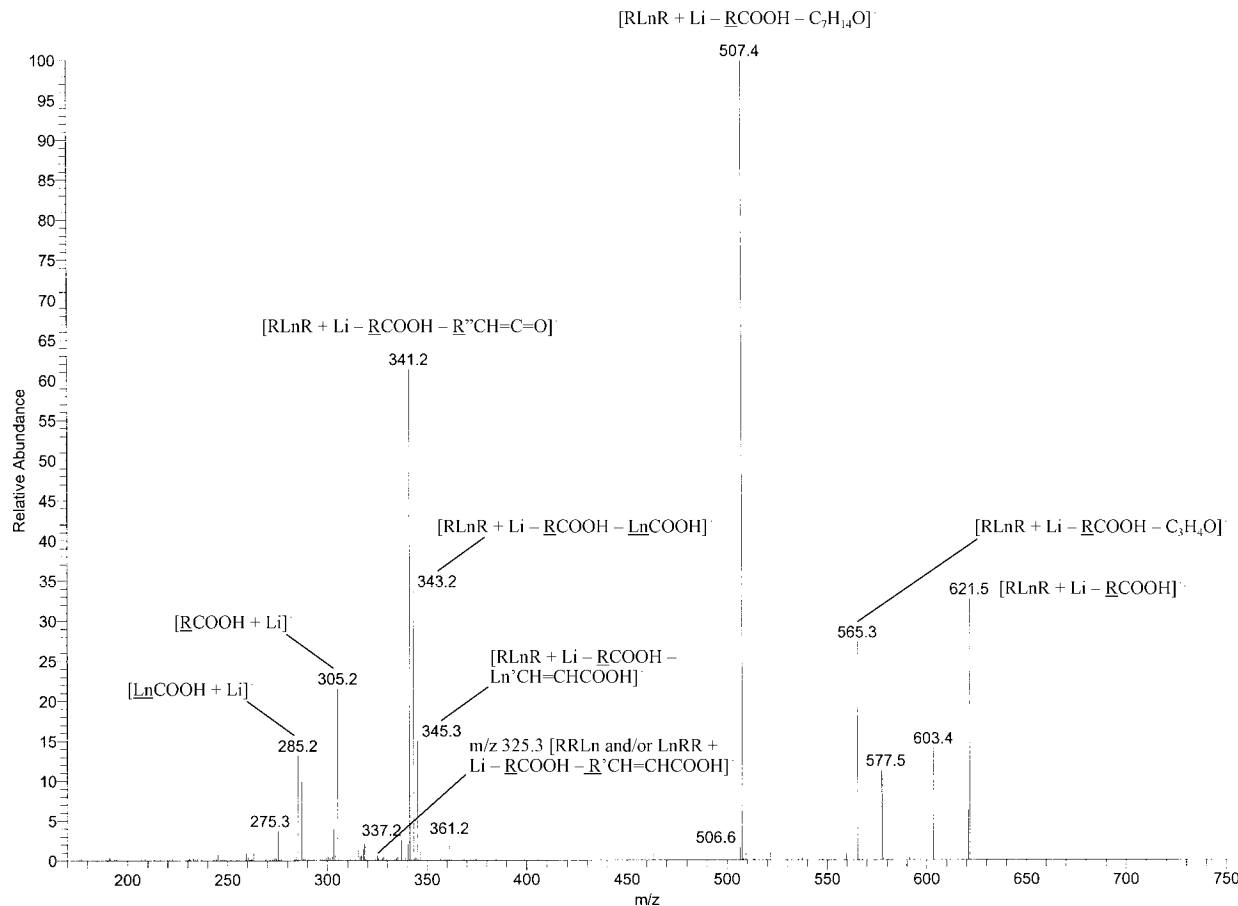


Figure 7. Ion trap mass spectrum of ESI-MS³ of $[\text{RLnR} + \text{Li} - \text{RCOOH}]^+$ at m/z 623.5. For abbreviations, see **Figures 2 and 3**. $\text{Ln}'\text{CH}=\text{CHCOOH}$ is α,β -unsaturated linolenic acid from the *sn*-2 position. Both Ln and $\text{Ln}'\text{COOH}$ are linolenic acid. RLnR here is diricinoleoyl-linolenoyl-glycerol (non-stereospecific) from castor oil including RRLn and LnRR if any.

fatty acids. Fatty acids are then activated to become acyl-CoA. Ricinoleoyl-CoA, linoleoyl-CoA, linolenoyl-CoA, and lesqueroloyl-CoA must come from the pathway involving PC, where hydroxylation and desaturation occur. Oleoyl-CoA, stearoyl-CoA, and palmitoyl-CoA can be available from the plastid. Acylation on the glycerol backbone by acyl-CoA can be at *sn*-1, *sn*-2, and *sn*-3 by different acylation steps on the pathway.

The contents of the five RACR containing non-hydroxyl acyl chains at the *sn*-2 position were high. This indicated that phospholipase A₂ hydrolysis of PC containing non-hydroxyl fatty acid at the *sn*-2 position is either blocked or partially blocked *in vivo* and these non-hydroxyl fatty acids stay mostly at *sn*-2 position of triacylglycerol in castor oil. It has been shown previously *in vitro* that ricinoleate was released specifically from PC by phospholipase A₂ in castor microsomes (17, 18). The lesqueroloyl moiety on the *sn*-2 position of diricinoleoyl-lesqueroloylglycerol represents about one-third of the three possible isomers, suggesting that 2-lesqueroloyl-PC, like 2-ricinoleoyl-PC, can be hydrolyzed by phospholipase A₂ efficiently. In addition, lysophosphatidic acid acyltransferase (acylation step on *sn*-2) may incorporate more non-hydroxyl fatty acids into castor oil than the acylation steps of lysophosphatidic acid acyltransferase (*sn*-1) and diacylglycerol acyltransferase (*sn*-3) combined.

In castor oil, non-hydroxyl fatty acids are mostly at the *sn*-2 position, whereas in seed oils lacking hydroxy fatty acid, unsaturated fatty acids are mostly at the *sn*-2 position. The incorporation of non-hydroxyl fatty acids into triacylglycerols,

for example, ROR and RLR, includes the enzymatic steps catalyzed by phospholipase C and DGAT. Down-regulation of DGAT will block the incorporation of both hydroxy and non-hydroxyl fatty acids into triacylglycerols, potentially affecting oil yield. Therefore, phospholipase C can be the target to block the incorporation of non-hydroxyl fatty acids into triacylglycerols to increase presumably the content of ricinoleate in transgenic seed oils.

LITERATURE CITED

- (1) Lin, J. T.; Turner, C.; Liao, L. P.; McKeon, T. A. Identification and quantification of the molecular species of acylglycerols in castor oil by HPLC using ELSD. *J. Liq. Chromatogr. Relat. Technol.* **2003**, *26*, 773–780.
- (2) Lin, J. T.; Woodruff, C. L.; Lagouche, O. J.; McKeon, T. A.; Stafford, A. E.; Goodrich-Tanrikulu, M.; Singleton, J. A.; Haney, C. A. Biosynthesis of triacylglycerols containing ricinoleate in castor microsomes using 1-acyl-2-oleoyl-*sn*-glycerol-3-phosphocholine as the substrate of oleoyl-12-hydroxylase. *Lipids* **1998**, *33*, 59–69.
- (3) Lin, J. T.; Lew, K. M.; Chen, J. M.; Iwasaki, Y.; McKeon, T. A. Metabolism of 1-acyl-2-oleoyl-*sn*-glycerol-3-phosphocholine in castor oil biosynthesis. *Lipids* **2000**, *35*, 481–486.
- (4) Lin, J. T.; Chen, J. M.; Chen, P.; Liao, L. P.; McKeon, T. A. Molecular species of PC and PE incorporated from free fatty acids in castor oil biosynthesis. *Lipids* **2002**, *37*, 991–995.

(5) Lin, J. T.; Arcinas, A.; Harden, L. A.; Fagerquist, C. K. Identification of (12-ricinoleoylricinoleoyl)diricinoleoylglycerol, and acylglycerol containing four acyl chains, in castor (*Ricinus communis* L.) oil by LC-ESI-MS. *J. Agric. Food Chem.* **2006**, *54*, 3498–3504.

(6) van de Loo, F. J.; Broun, P.; Turner, S.; Somerville, C. An oleate 12-hydroxylase from *Ricinus communis* L. is a fatty acyl desaturase homolog. *Proc. Natl. Acad. Sci. U.S.A.* **1995**, *92*, 6743–6747.

(7) Broun, P.; Somerville, C. Accumulation of ricinoleic, lesquerolic, and denipolic acids in seeds of transgenic *Arabidopsis* plant that express a fatty acyl hydroxylase cDNA from castor bean. *Plant Physiol.* **1997**, *113*, 933–942.

(8) Hsu, F.-F.; Turk, J. Structural characterization of triacylglycerols as lithiated adducts by electrospray ionization mass spectrometry using low-energy collisionally activated dissociation on a triple stage quadrupole instrument. *J. Am. Soc. Mass Spectrom.* **1999**, *10*, 587–599.

(9) Lin, J. T.; Woodruff, C. L.; McKeon, T. A. Non-aqueous reversed-phase high-performance liquid chromatography of synthetic triacylglycerols and diacylglycerols. *J. Chromatogr. A* **1997**, *782*, 41–48.

(10) Lin, J. T.; McKeon, T. A. Separation of the molecular species of acylglycerols by HPLC. In *HPLC of Acyl Lipids*; Lin, J. T., McKeon, T. A., Eds.; HNB Publishing: New York, 2005; Chapter 8, pp 199–220.

(11) Lin, J. T.; McKeon, T. A. Relative retention times of the molecular species of acylglycerols, phosphatidylcholines and phosphatidylethanolamines containing ricinoleate in reversed-phase HPLC. *J. Liq. Chromatogr. Relat. Technol.* **2003**, *26*, 1051–1058.

(12) Cheng, C.; Gross, M. L.; Pittenauer, E. Complete structural elucidation of triacylglycerols by tandem sector mass spectrometry. *Anal. Chem.* **1998**, *70*, 4417–4426.

(13) Mottram, H. R.; Woodbury, S. E.; Evershed, R. P. Identification of triacylglycerol positional isomers present in vegetable oils by high performance liquid chromatography/atmospheric pressure chemical ionization mass spectrometry. *Rapid Commun. Mass Spectrom.* **1997**, *11*, 1240–1252.

(14) Mottram, H. R.; Crossman, Z. M.; Evershed, R. P. Regiospecific characterization of the triacylglycerols in animal fats using high performance liquid chromatography–atmospheric pressure chemical ionization mass spectrometry. *Analyst* **2001**, *126*, 1018–1024.

(15) Jakab, A.; Jablonkai, I.; Forgacs, E. Quantification of the ratio of positional isomer dilinoleoyl-oleoyl glycerols in vegetable oils. *Rapid Commun. Mass Spectrom.* **2003**, *17*, 2295–2302.

(16) Byrdwell, W. C. The bottom-up solution to the triacylglycerol lipidome using atmospheric pressure chemical ionization mass spectrometry. *Lipids* **2005**, *40*, 383–417.

(17) Bafor, M.; Smith, M. A.; Jonsson, L.; Stobart, K.; Stymne, S. Ricinoleic acid biosynthesis and triacylglycerol assembly in microsomal preparation from developing castor bean (*Ricinus communis*) endosperm. *Biochem. J.* **1991**, *280*, 507–514.

(18) Stahl, U.; Banas, A.; Stymne, S. Plant microsomal phospholipid acyl hydrolases have selectivities for uncommon fatty acids. *Plant Physiol.* **1995**, *107*, 953–962.

Received for review October 27, 2006. Revised manuscript received January 12, 2007. Accepted January 15, 2007.

JF063105F